Inorganic Chemistry

ARTICLE

pubs.acs.org/IC

Visible-Light-Derived Photocatalyst Based on $TiO_{2-\delta}N_{\delta}$ with a Tubular Structure

Yoshikazu Hirose,[†] Toshinori Mori,[†] Yuka Morishita,[†] Atsushi Itadani,[†] Takayuki Kudoh,[‡] Takahiro Ohkubo,[†] Tomoko Matsuda,[§] Shigeharu Kittaka,[§] and Yasushige Kuroda*[,†]

[†]Department of Fundamental Material Science and [‡]Department of Medical and Bioengineering Science, Graduate School of Natural Science and Technology, Okayama University, 3-1-1 Tsushima, Kita-ku, Okayama 700-8530, Japan

[§]Department of Chemistry, Faculty of Science, Okayama University of Science, 1-1 Ridaicho, Kita-ku, Okayama 700-0005, Japan

Supporting Information

ABSTRACT: We succeeded in achieving visible-light responsiveness on a tubular TiO_2 sample through the treatment of a tubular TiO_2 that has a large surface area with an aqueous solution of ammonia or triethylamine at room temperature and subsequent calcination at 623 K, which produced a nitrided tubular TiO_2 sample. It was found that the ease of nitridation is dependent on the surface states; washing the tubular TiO_2 sample with an aqueous acidic solution is very effective and indispensable. This treatment causes the appearance of acidic sites on the tubular TiO_2, which was proved by the following experiments: NH_3 temperature-programmed desorption and two types of organic reactions exploiting the acid properties. The prepared samples, $TiO_{2-\delta}N_{\delta}$, efficiently absorb light in the visible region, and they exhibit a prominent feature for the decomposition of methylene blue in an aqueous solution at 300 K under irradiation with visible light, indicating the achievement of visible-light responsiveness on the tubular TiO_2 sample. This type of tubular $TiO_{2-\delta}N_{\delta}$ sample has merit in the sense that it has a large surface area and a characteristic high transparency for enabling photocatalytic reactions because it has a tubular structure and is composed of thin walls.

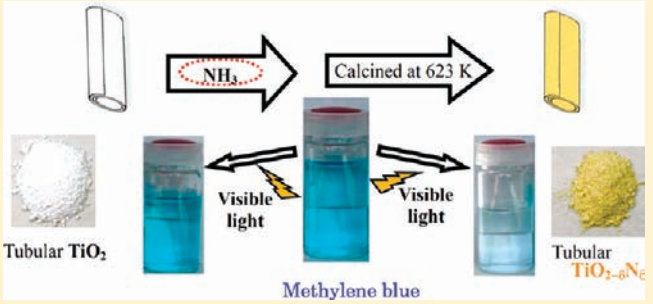

INTRODUCTION

Titanium dioxide (TiO_2) has received much attention recently as a promising material for use in photochemical applications as a photocatalyst since the discovery that water molecules or organic pollutants are decomposed on TiO_2 under ultraviolet (UV) irradiation.[1−5] TiO_2 has the advantages of being both inexpensive and nontoxic, in addition to its excellent functionality and long-term stability. However, TiO_2 becomes active in photoexcitation only under UV-light irradiation with energy greater than its band gap (about 3.2 eV).[3,4] Our ultimate purpose is to produce a photocatalyst that can operate efficiently under visible-light irradiation. The efforts have so far been directed toward developing visible-light-responsive materials by reducing the band gap of TiO_2; such approaches are accompanied by doping with impurities in the material. Samples that include metal impurities,[6−11] oxygen-deficient,[12,13] carbon,[14−17] nitrogen,[18−27] fluorine,[28−31] or sulfur,[17,32] as well as coupling with narrow-band-gap semiconductors,[33,34] have been prepared, and their sensitivities to visible light have been examined. In particular, the nitrogen-doped material has received much attention since Asahi et al. reported its activity by using a film-type material.[19] A visible-light-responsive TiO_2 powder sample is also potentially useful in photocatalytic reactions; hence, powdered nitrogen-doped titania is advantageous for practical use as a functional material.[35−45] Generally, the powdered or filmy nitrogen-doped TiO_2 sample is prepared by reaction with N_2 or NH_3 at high temperatures;[46−48] however, the samples thus prepared have a low surface area, as well as a rutile structure, causing lower reactivity in photocatalytic processes. Considering such circumstances, the preparation of titanium oxynitride, $TiO_{2-\delta}N_{\delta}$, having a larger surface area under wet or mild conditions is a very significant subject and presents advantages over various other methods.[18,49−53] From such viewpoints, it would be epoch-making if nitrogen doping onto the high-surface-area tubular TiO_2 was possible. Actually, it may become feasible to achieve such characteristics on a tubular TiO_2 by taking account of the recently reported result that this type of tubular sample exhibits a very unusual surface nature as an acid site.[54,55]

In this experiment, we succeeded in achieving visible-light responsiveness on tubular TiO_2 samples through the treatment of tubular TiO_2 that has a large surface area with an aqueous solution of ammonia or triethylamine (TEA) at room temperature and subsequent calcination at 623 K, according to the dependence of their reactivity on the surface states of the tubular sample. The photocatalytic properties of the respective tubular

Received: March 2, 2011
Published: September 12, 2011

dx.doi.org/10.1021/ic200424v | *Inorg. Chem.* 2011, 50, 9948–9957

samples were also examined for the photodegradation of methylene blue (MB), as a typical example.

EXPERIMENTAL SECTION

Sample Preparation. Tubular titania was synthesized by a hydrothermal treatment of a typical P-25 sample, TiO_2(P-25) (4 g), in an aqueous solution of NaOH (10 M, 100 cm^3); the hydrothermal treatment in a 150 cm^3 Teflon-lined autoclave was performed at 413 K for 72 h.[56−67] After the hydrothermal reaction, the precipitate obtained was thoroughly washed with distilled water until there was no further change in the pH value of the supernatant solution. The sample thus obtained, which shows a tubular structure, is abbreviated as T-TiO_2(W). The tubular sample prepared by treatment with NaOH was also immersed in an aqueous solution of 1 M acetic acid (HAC), followed by sonication. This washing process was repeated more than 10 times, and finally the product was washed thoroughly with distilled water to give T-TiO_2(AC). The T-TiO_2(AC) sample (4 g) was dispersed into distilled water (20 cm^3) under ultrasonic treatment conditions for 10 min. The resultant suspension was subsequently treated in an ultrasonic bath for 10 min by adding an aqueous solution of NH_3 (28 wt %, 40 cm^3), followed by drying at 303 K. The resultant precipitate was finally annealed at 623 K for 4 h in an atmosphere of dioxygen, resulting in the formation of a nitrogen-incorporated tubular sample, T-$TiO_{2-\delta}N_\delta$(NH_3). Similar samples having different amounts of doped nitrogen in T-TiO_2 were prepared by treating the T-TiO_2(AC) sample with TEA; the T-TiO_2-(AC) sample was dispersed in an aqueous solution (100 cm^3) including 1.0 (or 5.0) wt % TEA, followed by sonication for 10 min. Then, the prepared materials were dried at 303 K for 24 h, followed by calcination at 623 K for 4 h. These samples are abbreviated as T-$TiO_{2-\delta}N_\delta$(TEA01) and T-$TiO_{2-\delta}N_\delta$(TEA05), respectively. The TiO_2 sample that was obtained by hydrolysis of titanium isopropoxide with an aqueous solution of NH_3 and subsequently calcined at 623 K was used as the reference sample, abbreviated as TiO_2(hydrolysis-NH_3).[23]

Transmission Electron Microscopy (TEM) and X-ray Diffraction (XRD) Measurements. All samples were imaged with a JEOL JEM-2010F transmission electron microscope equipped with a LaB_6 crystal for electron generation. A few milligrams of each sample were suspended in methanol, and the solution was dispersed by sonication for 5 min. A drop of this solution was then placed on a TEM grid (copper grid covered with electric arc-deposited carbon) and allowed to dry in air under a lamp. For image acquisition, the applied voltage was set between 80 and 200 keV.

Phase and crystallinity identifications of the tubular samples were performed with powder XRD using a Rigaku diffractometer (MiniFlexII) with Cu Kα radiation (λ = 1.541 84 Å) under the operating conditions of 30 kV and 15 mA.

Diffuse-Reflectance (DR) Spectral Measurements. UV−vis−near-IR DR spectra were recorded at 300 K in the wavelength range of 200−2500 nm using a spectrophotometer (Jasco V-570) equipped with an integral sphere attachment to obtain the DR spectra of the samples. The powdered sample was placed in a vacuum reflectance cell made of fused silica. The samples were evacuated at various temperatures under in situ conditions without exposure to environmental gases. Spectralon (Labsphere USA) was used as the reference material.

IR Spectral Measurements. Fourier transform infrared (FTIR) spectroscopic measurements were performed at 300 K by accumulating 64 scans at a nominal resolution of 2 cm^{-1}, using a Digilab FTS-4000MXK FTIR spectrophotometer equipped with a triglycine sulfate detector. The sample was pressed into pellets with 10 mm diameter and placed in an in situ cell capable of withstanding pretreatment at high temperatures and adsorption−desorption (evacuation) operations in the in situ condition. First, the sample was evacuated at various temperatures, subjected to treatment with dioxygen under an equilibrium pressure of 1.3 kPa, and then exposed to NH_3 vapor, followed by evacuation at the chosen temperatures. The equilibrium pressure of the adsorbing gas was monitored with an MKS Baratron-type 390 B transducer.

Raman Spectral Measurements. Raman scattering measurements were performed in the backward-scattering geometry using a Ventuno 21 NRS-1000 instrument (Jasco) at room temperature. The Raman spectra were accumulated 32 times from 40−1200 cm^{-1} with a slit width of 300 μm and a spectral resolution of 14.09 cm^{-1}. The 532.0 nm line of a solid laser (Nd:YVO_4 with a nonlinear optical crystal inside the laser cavity) was used for excitation at a power level of 100 mW. The spectrometer was equipped with a CCD camera detector.

X-ray Photoelectron Spectroscopy (XPS) Measurements. XPS measurements were carried out using the advanced XPS imaging spectrometer AXIS-HS (Shimadzu) with a Mg Kα source to analyze the surface states, especially the states of doped nitrogen, of various samples. An electron gun was used to neutralize the surface charging occurring for insulated samples. Because of a carbonaceous residue on the samples, the peak of C_{1s} at 284.8 eV was used for internal calibration of the energy scale. All samples were first degassed at 300 K under a reduced pressure of 1.3×10^{-7} Pa. The nitrogen amounts doped in the various samples were evaluated based on the data reported by Wagner et al.[68]

N_2 Adsorption and Desorption Isotherm Measurements. The pore structures and surface areas of the samples were determined from N_2 adsorption and desorption isotherms at 77 K using an automatic adsorption apparatus (BEL Japan, Inc., type BELSORP-max). Prior to adsorption of N_2, each sample was degassed at 343 K for 4 h. The surface areas of the samples were evaluated by applying the obtained isotherms to the Brunauer−Emmett−Teller equation. The pore-size distribution was calculated from the adsorption branch using the Barrett−Joyner−Halenda method.

Temperature-Programmed Desorption (TPD) Measurements. TPD experiments were performed using a BELCAT-A apparatus (BEL Japan, Inc.) with a thermal conductivity detector (TCD) based on a typical four-element tungsten−rhenium filament and/or a mass spectrometer (BELMass) using a quadrupole mass analyzer as the detector. In each TPD measurement, the samples were first purged by helium (flow rate: 50 mL min^{-1}) at 300 K for 2 h, with the conditions for the TPD measurements being as follows: helium was used as the carrier gas at a rate of 30 mL min^{-1}, and the heating rate was 10 K min^{-1} to 873 K.

Degradation Reaction of MB. The photocatalytic activity of each sample was tested by the degradation of MB. An amount of 10 mg of photocatalyst was calcined at 623 K for 6 h and then dispersed in 100 cm^3 of a MB aqueous solution (2.0×10^{-5} M). The mixture was stirred for 1 h in the dark and then filtered. These operations were repeated to reach MB adsorption equilibrium on the photocatalyst. Then, the sample, which had completely adsorbed MB, was dispersed in 30 cm^3 of a MB aqueous solution (1.0×10^{-5} M). The photocatalytic reaction was performed in a quartz reactor irradiated by a 100 W xenon light source (Asahi spectra, LAX-Cute). To limit the irradiation wavelengths, the light beam was passed through a Y-44 filter (Hoya Candeo Optronics) to obtain a wavelength range of 440−700 nm. After the mixture was irradiated for 1 h, the catalyst was recovered by filtering, and the light absorption of the solution was measured with a UV−vis spectrophotometer (Jasco V-550).

RESULTS AND DISCUSSION

1. Recognition of the Surface Acidic Properties of the Prepared Tubular Sample. Surface characterization of the tubular TiO_2 sample T-TiO_2(AC), which has an acidic nature, is essential to examine the reactivity for nitridation of this sample by utilizing simple molecules with a basic nature, such as ammonia and TEA.[54,55] The TPD experimental procedure is appropriate to determine the surface acidic properties.[55,69] The

dx.doi.org/10.1021/ic200424v |Inorg. Chem. 2011, 50, 9948–9957

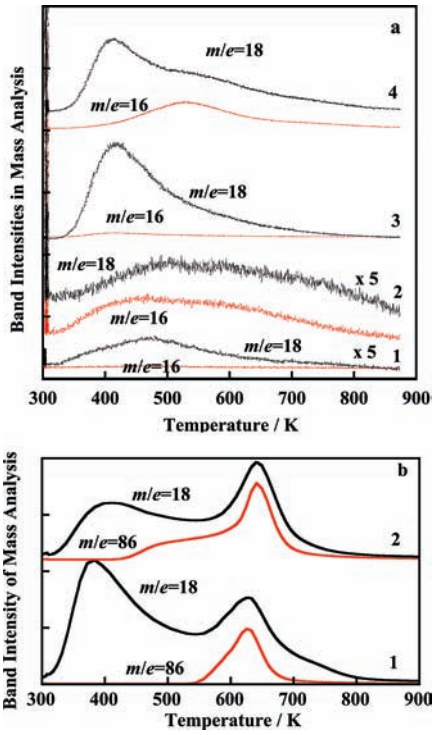

Figure 1. (a) TPD-MS spectra for H_2O and NH_3 of the respective samples: (1) TiO_2(P-25); (2) NH_3-adsorbed TiO_2(P-25); (3) T-TiO_2-(AC); (4) T-$TiO_{2-\delta}N_\delta(NH_3)$. Each sample had been dried at 300 K. In this graph, the spectra for samples 1 and 2 are multiplied by 5 in *y* values of the original data. (b) TPD-MS spectra for H_2O and $N(C_2H_5)_3$ of the respective samples: (1) T-$TiO_{2-\delta}N_\delta$(TEA01); (2) T-$TiO_{2-\delta}N_\delta$-(TEA05). Both samples had been dried at 300 K.

amount and number of different types of surface acidic sites can be evaluated based on this measurement. Ammonia was selected as a probe molecule because it is used as the reactant for nitridation of the tubular TiO_2 sample in this experiment and also is recognized as a suitable compound by taking into account the size of the molecule. In the present case, it is expected that a large amount of water also exists on the surface, simultaneously with ammonia. Therefore, great difficulty will be encountered in a TPD experiment utilizing the TCD method because of the simultaneous desorption of both H_2O and NH_3 from the T-TiO_2(AC) sample treated with ammonia. To avoid such a problem, we used the mass analysis method for detection of the respective gases. In this experiment, mass numbers of 16 and 18 were utilized for detection of the respective molecules, by taking account of the cross section of NH_3 and H_2O. In the present case, two types of dominant desorption bands are observed in the TPD because of H_2O and NH_3 for the NH_3-treated sample, T-$TiO_{2-\delta}N_\delta(NH_3)$, as shown in Figure 1: the band centered at around 423 K is due to desorbed H_2O, which shows a shoulder toward higher temperature and a band at around 533 K for NH_3, which exhibits a symmetrical desorption nature. The TPD spectra observed are also given in Figure S1 in the Supporting Information, in which a TCD was used as the detector. The observed tendencies are very consistent with the desorption behavior observed by the IR method (1435 cm^{-1} band, described below). For the T-TiO_2(AC) sample, the latter band in TPD-mass spectrometry (MS) spectra (due to NH_3) is hardly observed and only the former band (due to H_2O) was found. As for the TiO_2(P-25) sample, two types of bands were observed at 400 and 473 K, which are ascribable to the desorbed H_2O, although both components are smaller in amount compared with the band intensity for the tubular sample. Needless to say, there is no band due to NH_3 species for the T-TiO_2(AC) and TiO_2(P-25) samples. In addition, it is noteworthy that, even after the NH_3 adsorption on TiO_2(P-25), the desorbed NH_3 gas was detected in small quantity and the desorption temperature is lower than that observed for the NH_3-treated T-TiO_2(AC) sample, as shown in the spectrum 2. As for the acidity, the present sample, T-TiO_2(AC), showed slightly weaker Brønsted or Lewis acidity than those for various types of H-zeolite samples,[70] although its acidity is definitely higher than that observed for ordinary TiO_2 samples, such as TiO_2(P-25). In addition, we also examined a similar experiment utilizing TEA as a probe molecule for samples treated with an aqueous solution of 1.0 and 5.0 wt % TEA because this molecule is also used as an agent for nitridation in this experiment. In this case, the mass number of 86 from the parent peak of TEA was selected for the detection of desorbed species. The resultant data are also depicted in Figure 1b. The specific feature for both samples was obtained as follows. In these cases, the desorption temperature is higher than that observed for the T-TiO_2(AC) sample treated with ammonia, indicating stronger interaction of the surface of the T-TiO_2(AC) sample with TEA, reflecting the more basic nature of TEA compared with ammonia.

To determine the acidic nature of the T-TiO_2(AC) sample, we examined the catalytic performance through two types of reactions: the ring-opening reaction of epoxide and a Friedel−Crafts-type reaction. The detailed experimental procedures are given in the Supporting Information. For comparison, the same reactions were also carried out utilizing the starting material TiO_2(P-25), as well as the commercial silica, Aerosil 200, and the MCM-41 sample prepared in our laboratory.[71] The present inorganic solid acid, T-TiO_2(AC), is expected to possess a Brønsted acid site that plays a crucial role in determining the catalytic activity for these reactions because such reactions proceed efficiently over a Brønsted acid catalyst. In the first reaction (ring-opening reaction of epoxide), the lone-pair electrons on the O atom in a styrene oxide molecule were protonated through attack by H^+ arising from a Brønsted acid site, followed by attack by the nucleophilic part of methanol onto this carbon center, resulting in the ring-opening reaction, as shown in Scheme 1a. Another type of reaction (Friedel−Crafts-type) was started by activation of the CO group in methyl vinyl ketone through protonation, followed by attack by the π electrons in indole upon the vinyl group (Scheme 1b). The results show that the T-TiO_2(AC) sample exhibits remarkably high catalytic performance for the reactions even at 300 K, with the data being given in Table 1. In the first reaction, the yield evaluated for T-TiO_2(AC) is 73%, that for TiO_2(P-25) is 10%, that for Aerosil 200 is lower than 2%, and that for MCM-41 is only a trace amount. As for the second reaction, the yield reached 94% in shorter reaction times for T-TiO_2(AC), in contrast to the silica catalysts (5% and 3%), as well as the starting material, TiO_2(P-25), 17%. From these data, it is obvious that the T-TiO_2(AC) sample has an acidic nature, although the details of the mechanism for the appearance of this acidic nature are not clear at the present stage.

2. Verification of the Formation of Nitrided Tubular TiO_2 Samples. Figure 2 shows the DR spectra for typical samples, TiO_2(P-25), T-TiO_2(AC), TiO_2(hydrolysis-NH_3), T-$TiO_{2-\delta}$-$N_\delta(NH_3)$, T-$TiO_{2-\delta}N_\delta$(TEA01), and T-$TiO_{2-\delta}N_\delta$(TEA05),

dx.doi.org/10.1021/ic200424v |*Inorg. Chem.* 2011, 50, 9948–9957

Scheme 1

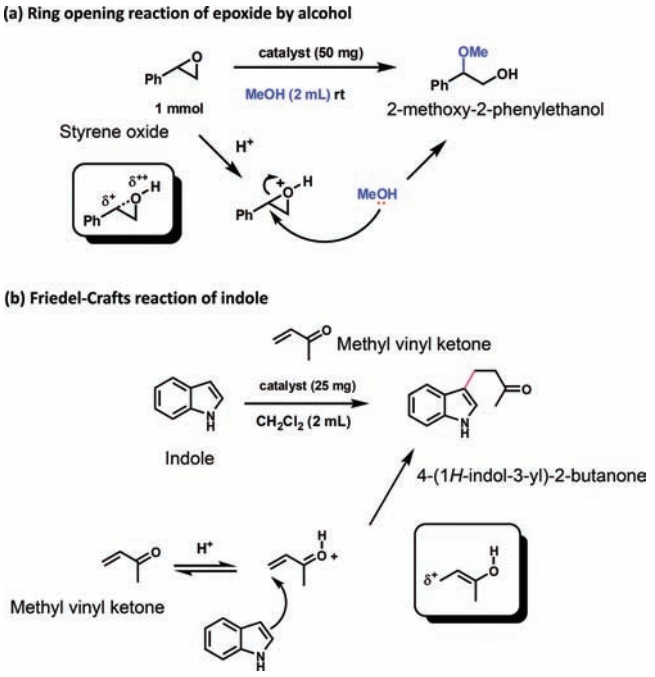

Table 1. Reaction Yields Obtained for the Respective Reactions Tested on the TiO_2 and SiO_2 Samples

	reaction 1		reaction 2	
catalyst	yield (%)	time	yield (%)	time
T-TiO_2 (AC)	73	4 h	94	2 days
TiO_2(P-25)	10	3 days	17	6 days
MCM-41	trace	50 h	3	3 days
Aerosil 200	<2	48 h	5	5 days

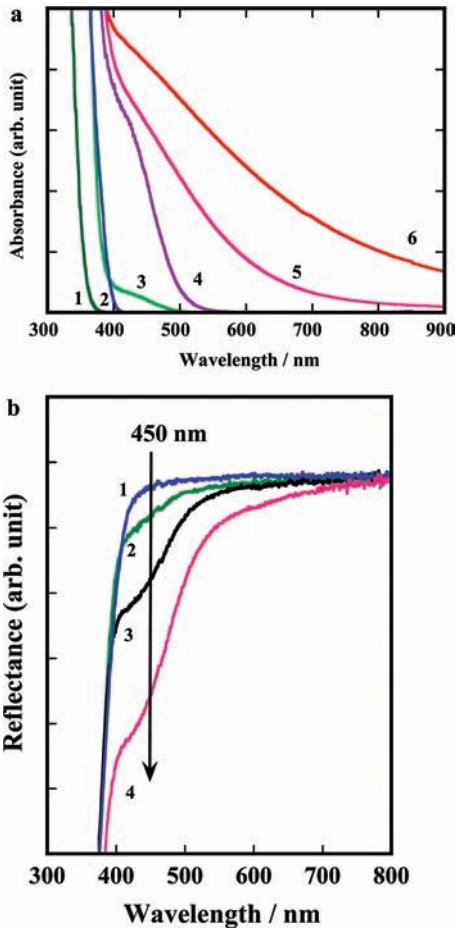

Figure 2. (a) DR spectra of the TiO_2 samples. All spectra were measured after calcination of the respective samples at 623 K: (1) T-TiO_2(AC); (2) TiO_2(P-25); (3) TiO_2(hydrolysis-NH_3); (4) T-$TiO_{2-\delta}N_\delta$(NH_3); (5) T-$TiO_{2-\delta}N_\delta$(TEA01); (6) T-$TiO_{2-\delta}N_\delta$(TEA05). (b) DR spectra of the samples (T-TiO_2) that had been washed with an aqueous solution of HAC in different times (1) 0, (2) 2, (3) 6, and (4) 10 and then treated with an aqueous solution with ammonia, followed by evacuation at 623 K, and successively treated with dioxygen (1.3 kPa) at 623 K. To understand easily the change in the spectra, the *y* axis in this figure is represented by reflection, as is different from that given in Figure 2a.

which were measured at room temperature after calcination at 623 K. It is well-known that TiO_2 is generally obtained as a white powder having a band-gap energy of ca. 3.2 eV;[3,4] both T-TiO_2(AC) and TiO_2(P-25) samples only absorb light with a wavelength shorter than 400 nm (spectra 1 and 2). In addition, it is clearly indicated that the tubular sample has a larger band gap than TiO_2(P-25). A weak shoulder band between 400 and 500 nm was observed for the TiO_2(hydrolysis-NH_3) that had been calcined at 623 K, although the band in this region has a weak intensity (spectrum 3).[23] The as-prepared T-$TiO_{2-\delta}N_\delta$(NH_3) sample, which was prepared by just treating the T-TiO_2(AC) sample with an aqueous solution of NH_3 at room temperature, gave a white powder with no absorption in the visible-light region. In comparison, the T-$TiO_{2-\delta}N_\delta$(NH_3) sample calcined at 623 K was obtained as a pale-yellow powder. Corresponding to this fact, this pale-yellow sample exhibits a characteristic shoulder band in the region between 400 and 550 nm, which is clearly distinct from the cases of the calcined TiO_2(P-25) and T-TiO_2(AC), indicating the possibility of using this NH_3-treated material as a visible-light-sensitive photocatalyst (spectrum 4). The present data clearly indicate the superiority of this sample as an absorbent for visible light over the original samples, namely, both TiO_2(P-25) and T-TiO_2(AC), as well as TiO_2(hydrolysis-NH_3). This tendency is further enhanced by treatment with TEA, as can be seen in spectra 5 and 6. As a result, we can easily tune the amounts of nitrogen doped in T-$TiO_{2-\delta}N_\delta$ using various reagents having different donating power for nitridation.

First, to achieve more efficient nitrogen doping in the T-TiO_2 sample, we examined the effect of the surface state on the ease of nitridation. The tubular sample just prepared by treatment with NaOH was immersed in an aqueous solution of 1 M HAC, followed by sonication, as described in the Experimental Section. This washing process was repeated more than 10 times. Then, the prepared samples were treated with an aqueous solution of ammonia, followed by calcination at 623 K. Variation in the DR spectra with the number of washings is shown in Figure 2b. For easy understanding of the changes in the spectra, the *y* axis of the DR spectra is given in reflection mode in this figure. The appearance of a new band in the visible absorption region for

dx.doi.org/10.1021/ic200424v |*Inorg. Chem.* 2011, 50, 9948–9957

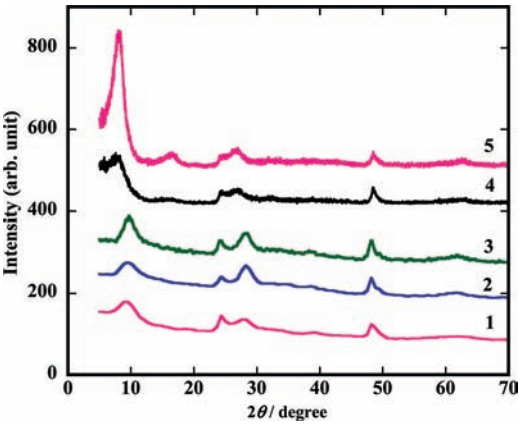

Figure 3. XRD data for the respective samples: (1) T-TiO_2(W); (2) T-TiO_2(AC); (3) T-$TiO_{2-\delta}N_\delta(NH_3)$; (4) T-$TiO_{2-\delta}N_\delta$(TEA01); (5) T-$TiO_{2-\delta}N_\delta$(TEA05).

the calcined samples at 623 K is ascribable to the doping of nitrogen in the TiO_2 lattice as well as on the surface, i.e., to the appearance of impurity levels in the band-gap regions composed of O and Ti ions (see also a later section for a discussion of the XPS data).[19] By comparison with the observed spectra, it is clearly seen that the washed sample exhibits high responsiveness for visible light with an increase in the number of washings with an aqueous solution of HAC, indicating the possibility of the greater effectiveness of the photocatalytic reaction making use of the light in the visible absorption region, because it is expected that the prepared sample has almost similar crystallinity and the starting material is the same. The differences in the surface states with variation of the number of washings were also checked by the IR spectra using CO as a probe molecule, with the spectra being given in Figure S2 in the Supporting Information. Considering the results of DR and IR spectral measurements, it is reasonable to infer that the sites formed through the treatment at higher temperatures, which behave as Lewis acid sites giving the 2195 cm^{-1} band for the adsorbed CO species, act as reaction centers for the NH_3 molecules, causing insertion of the N atoms into the lattice.

The observed XRD pattern of the tubular sample prepared in this work was very consistent with that obtained for the tubular TiO_2 sample reported by Kasuga et al.;[56,57] the well-defined diffraction bands from the lower angle are ascribable to the diffractions from the (001), (110), (211), and (020) planes (Figure 3, as one of the assignments).[56−62] The samples treated with HAC, followed by treatment with NH_3 or TEA, also give a pattern similar to that for the original sample, indicating that these samples retain their tubular structure. In the case of the TEA-treated samples, the diffraction from the (001) plane is shifted toward a lower angle. This is ascribable to the expansion of the layers composed of titanate because of intercalation of both TEA and H_2O into the layers. This fact may be explained by considering the results obtained by TPD data; a large amount of water also desorbed simultaneously with TEA.

On the basis of the data described above, the N_2 adsorption data were also measured to obtain fundamental information on the pore structure of these samples. The N_2 adsorption−desorption isotherms for the samples before and after calcination at 623 K revealed type II isotherms; all isotherms measured reflected a similar type of isotherm, although the adsorbed amounts were slightly different, depending on the treatment temperatures of the samples (all isotherms and pore-size-distribution results are given in the Supporting Information, Figure S3). The specific surface areas and pore diameters are summarized in Table 2. All samples evacuated at 300 K give larger surface areas of ca. 300 m^2 g^{-1}, which agrees well with the considerations derived from the XRD data, i.e., the formation of tubular-type samples. This type of isotherm exhibits a nature similar to that observed for the original samples even after heat treatment at 623 K, although a decrease in the surface area to ca. 250 m^2 g^{-1}, being far larger than that for P-25 (ca. 50 m^2 g^{-1}), was observed.[72] From these data, we postulate that different nitrided samples were prepared while maintaining the tubular morphology.

Raman measurements for the samples were also carried out, and the spectra are given in the Supporting Information (Figure S4). The band characteristics of the tubular structure (181, 274, 397, 455, 663, 835, and 930 cm^{-1}) were also found in all spectra, supporting retention of the tubular structure for all samples prepared in this experiment, even after calcination at 623 K.[67,73−75] We must say that some crystallization (to the anatase phase) occurs after calcination at 623 K of the TEA-treated sample by taking account of the Raman data.

To verify our deduction, we performed TEM measurements on the samples. Figure 4 shows TEM images of T-TiO_2(AC) used in this experiment as the starting material, the ammonia-treated TiO_2 sample [T-$TiO_{2-\delta}N_\delta(NH_3)$], and the TEA-treated sample [T-$TiO_{2-\delta}N_\delta$(TEA05)], before and after calcination at 623 K. The shape of the starting material, which was prepared by hydrothermal treatment of the TiO_2(P-25) sample in an aqueous solution of NaOH, was needlelike, in which a tubular structure of ca. 5 nm diameter with a wall thickness of 2 nm was clearly seen. This structure was retained after washing with HAC. The tubular structure of this sample was completely maintained after treatment with an aqueous solution of ammonia or TEA at room temperature. The tubular structure of the respective samples was basically retained even after treatment at 623 K, although some amorphous phases could be seen in the samples treated at this temperature. The presence of some layered structure was observed in the position forming the wall in the sample. It was therefore realized that the tubular structure was made up of the wound titanate layer structure. As a result, it has become apparent that nitridation was performed for the tubular sample (T-TiO_2) while keeping its structure. This tendency was also the same for the samples treated with TEA. In this case [especially the T-$TiO_{2-\delta}N_\delta$(TEA05) sample], some black regions can be seen that may be due to the existence of the crystallized part; i.e., some crystallization occurred. As shown in Table 2, the surface areas of the respective T-TiO_2(AC) samples were 370 and 230 m^2 g^{-1}, clearly supporting the formation of the tubular sample and preservation of this structure even after treatment at high temperatures. Similar tendencies are also observed for the tubular samples treated with NH_3 or TEA; the tubular structure was preserved even after calcination at 623 K. A tubular TiO_2 sample has merit in the sense that it has a larger surface area and a characteristic high transparency for promoting reactions because it has a tubular structure and is composed of thinner walls. Finally, it should also be noted that TEM, Raman, and pore structural analysis data may indicate some crystallization occurring in the TEA-treated samples after calcination at 623 K, especially in the sample treated with a 5 wt % solution.

XPS was measured to determine the states of the nitrided T-TiO_2 samples, shown in Figure 5, together with those for T-TiO_2(W) and T-TiO_2(AC). First, the T-$TiO_{2-\delta}N_\delta(NH_3)$

dx.doi.org/10.1021/ic200424v |*Inorg. Chem.* 2011, 50, 9948–9957

Table 2. Surface Areas and Pore Sizes Giving the Maximum Values for Various Types of Tubular TiO_2 and Nitrided Samples

	evacuated at 300 K		calcined at 623 K, followed by evacuation at 300 K	
T-TiO_2 sample	surface area/m^2 g^{-1}	pore diameter/nm	surface area/m^2 g^{-1}	pore diameter/nm
T-TiO_2(AC)	371	4 and 20	226	ca. 4 and 20
T-$TiO_{2-\delta}N_\delta(NH_3)$	343	4 and 10—20	249	4 and 20
T-$TiO_{2-\delta}N_\delta$(TEA01)	318	4 and 10—25	263	20
T-$TiO_{2-\delta}N_\delta$(TEA05)	264	3—4 and 10	248	4 and 10

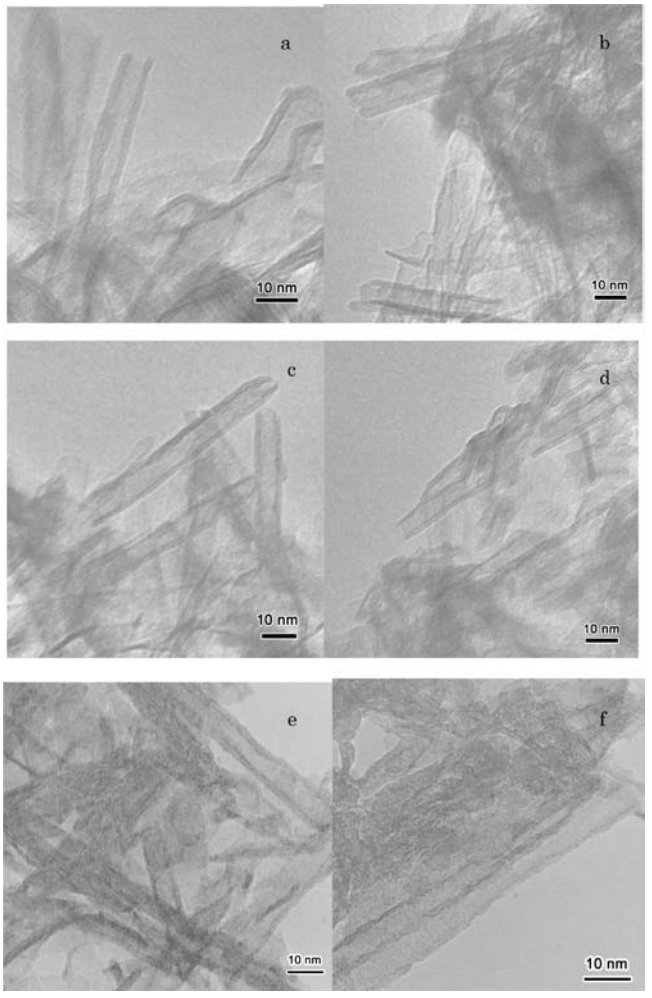

Figure 4. TEM images for the respective samples: (a and b) T-TiO_2-(AC); (c and d) T-$TiO_{2-\delta}N_\delta(NH_3)$; (e and f) T-$TiO_{2-\delta}N_\delta$(TEA05). (a, c, and e) As-prepared sample (before calcination); (b, d, and f) after calcination at 623 K.

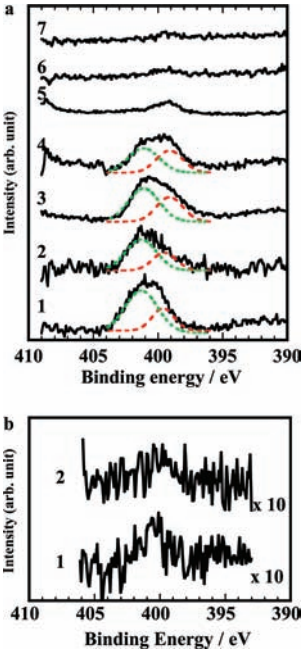

Figure 5. (a) N_{1s} XPS spectra for the $TiO_{2-\delta}N_\delta(NH_3)$ sample in the evacuation and successively dioxygen-treated stages: (1) 300 K, (2) 373 K, (3) 473 K, (4) 573 K, (5) 623 K, (6) 673 K, and (7) 723 K. (b) N_{1s} XPS spectra for the (1) T-TiO_2(W) and (2) T-TiO_2(AC) samples, which were evacuated at 300 K.

sample was calcined at various temperatures. For the sample treated at 300 K, a broad band assignable to N_{1s} was observed at around 400 eV, which is represented by the binding energy as the x axis. The observed band was separated into two dominant components by a curve-fitting procedure, assuming Gaussian functions centered at 401.4 and 399.6 eV. With increasing treatment temperatures, the former band loses its intensity compared with the intensity of the latter band. The assignment of XPS features in the NH_3-treated T-TiO_2(AC) sample, however, is still under debate, and controversial hypotheses are found in the literature.[19,20,22,24,26,27,41,46,68,76−90] In the case of nitrogen substitution for the oxygen in TiO_2, the electron density around nitrogen will be reduced, compared with that in TiN.[80] Therefore, the N_{1s} binding energy in N−Ti−O is higher than that in a N−Ti−N component. Taking into account both these points and the IR assignment (shown below), we tentatively assigned the former band to NH_4^+ or nitride species (interstitial N−Ti−O) and the latter to coordinated NH_3, NH_2 species, or nitrided species (substituted N−Ti−O).[86,87] The band at around 400 eV "survived" even after calcination at higher temperatures than 623 K, indicating that nitridation of the T-TiO_2 sample was verified. In addition, our assignment of the observed band at around 400 eV as the nitrogen species substituted for the oxygen in the initial O−Ti−O structure is in good agreement with the conclusion independently reported by Sathish et al.,[86] Di Valentin et al.,[87] Chen and Burda,[82] and Wang et al.,[90] although there are some controversies on the assignment of the state of the nitrogen species formed in TiO_2. From this evidence, one may say that the presence of the substituted nitrogen species was demonstrated by this experiment.

The N_{1s} XPS spectra for the respective nitrided samples, followed by calcination at 623 K, are also given in Figure 6, together with the results of the curve fitting, and the relative areas

dx.doi.org/10.1021/ic200424v |*Inorg. Chem.* 2011, 50, 9948–9957

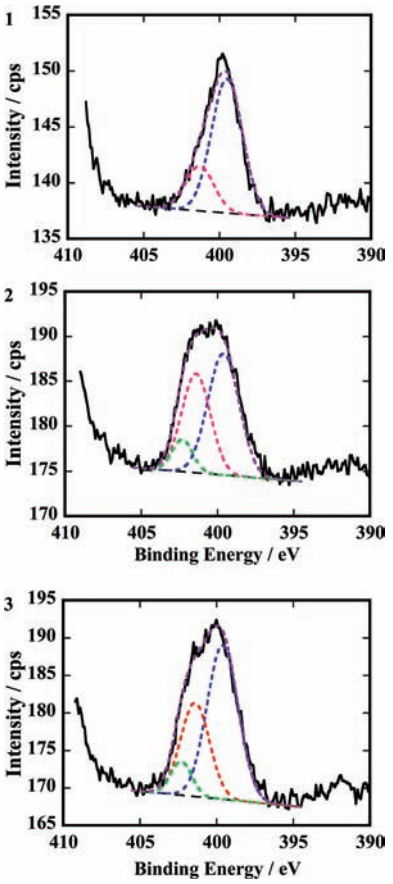

Figure 6. N_{1s} XPS spectra for various kinds of $TiO_{2-\delta}N_\delta$ samples that were prepared by calcination at 623 K after nitridation with NH_3 or TEA with different concentrations: (1) T-$TiO_{2-\delta}N_\delta(NH_3)$; (2) T-$TiO_{2-\delta}N_\delta$-(TEA01); (3) T-$TiO_{2-\delta}N_\delta$(TEA05).

Table 3. Relative Band Areas of the Respective Bands Being Ascribable to N_{1s} to the Band Observed at 399.6 eV for the T-$TiO_{2-\delta}N_\delta(NH_3)$ Sample

	band (399.6 eV)	band (401.4 eV)	band (402.3 eV)
T-$TiO_{2-\delta}N_\delta(NH_3)$	1	0.31	
T-$TiO_{2-\delta}N_\delta$(TEA01)	1.13	0.84	0.64
T-$TiO_{2-\delta}N_\delta$(TEA05)	1.71	0.95	0.82

for the respective bands of the 623 K treated samples are given in Table 3. In addition, the atomic ratios (atom %) for the 623 K treated samples were evaluated from the XPS data (Table 4). In this calculation, the procedures were as follows. First, the relative band areas were estimated based on the intensity of the band resulting from the Ti-$2P_{3/2}$ species. Second, the atomic ratios for Ti, O, and N elements were calculated by utilizing the relative cross-sectional values for Mg Kα radiation.[68]

Finally, we mention the small component found at around 402 eV after deconvolution of the spectra. It is well-known that nitrogen oxides give the N_{1s} bands in a wide region on the basis of experimental as well as literature assignments. Hyponitrite gives a band at 400 eV, whereas nitrite ion gives a band on the higher-energy side and another species, NO_3^-, also gives a band at around 407 eV.[88] Taking these data into consideration, the small component observed after deconvolution at around 402 eV may be assignable to the NO species or some oxidized species formed on the surface or in the bulk.[90]

Table 4. Relative Element Ratios (atom %) and Composition Ratios Based on Titanium, Given in Parentheses[a]

	Ti	O	N
T-$TiO_{2-\delta}N_\delta(NH_3)$	30.7 (1)	68.4 (2.23)	0.93 (0.030)
T-$TiO_{2-\delta}N_\delta$(TEA01)	30.5 (1)	68.0 (2.23)	1.53 (0.050)
T-$TiO_{2-\delta}N_\delta$(TEA05)	30.5 (1)	67.4 (2.21)	2.09 (0.068)

[a] Photoionization cross sections of respective elements were obtained from ref 68.

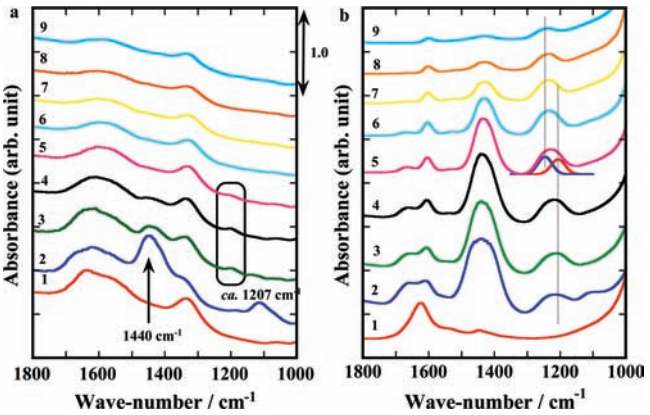

Figure 7. IR spectra for (a) T-TiO_2(W) and (b) T-TiO_2(AC) samples. The samples were evacuated at 473 K and then exposed to NH_3 under the pressure of 1.3 kPa, followed by evacuation and subsequent oxidation at increasing temperatures: (1) evacuation and subsequent oxidation at 473 K; (2) exposure to NH_3, followed by evacuation and subsequent oxidation at the respective temperatures (3) 300 K, (4) 323 K, (5) 373 K, (6) 423 K, (7) 473 K, (8) 523 K, and (9) 573 K.

3. Nitridation Process Utilizing the Peculiar Surface Properties of Tubular TiO_2 Samples. To explore the formation process of the visible-light-responsive tubular titanium oxynitride (or nitride) sample (T-$TiO_{2-\delta}N_\delta$), the IR spectra, which are given in Figure 7, were measured for both T-TiO_2(W) and T-TiO_2(AC) samples, which exhibited different reactivity in an aqueous ammonia solution, as described above. In particular, to obtain information on the relationship between the surface states of the samples and their reactivity with ammonia, we examined the IR spectra in the adsorption and reaction processes of NH_3 for both samples through treatment with gaseous NH_3, followed by evacuation and subsequent oxidation processes. For the original T-TiO_2(W) sample, three dominant IR bands were observed at around 1620, 1550, and 1330 cm^{-1}. The first band is assigned to the H_2O bending mode, and the others are due to carbonate species formed in the preparation process because the preparation of the sample was carried out under strongly basic conditions. Exposure to NH_3, followed by evacuation at 300 K, brings about four additional weak bands at 1656, 1605, 1440, and 1207 cm^{-1}. The bands at 1656 and 1440 cm^{-1} are due to the formed NH_4^+ species {the symmetric bending of NH_4^+ [$\delta_s(NH_4^+)$] and the asymmetric bending of NH_4^+ [δ_{as}-(NH_4^+)], respectively}; the other two bands at 1605 and 1207 cm^{-1} are due to coordinated NH_3 species {the asymmetric bending mode of NH_3 [$\delta_{as}(NH_3)$] and the symmetric bending

dx.doi.org/10.1021/ic200424v |Inorg. Chem. 2011, 50, 9948–9957

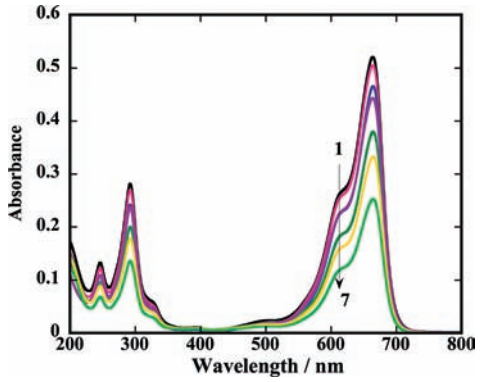

Figure 8. Degradation processes of MB on respective TiO_2 samples, which had been calcined at 623 K, under irradiation of visible light at 300 K: (1, black) an aqueous solution of MB kept under similar conditions; (2, red) TiO_2(P-25); (3, blue) T-TiO_2(AC); (4, violet) $TiO_{2-\delta}N_\delta$-(hydrolysis-NH_3); (5, dark green) T-$TiO_{2-\delta}N_\delta(NH_3)$; (6, yellow) T-$TiO_{2-\delta}N_\delta$(TEA01); (7, light green) T-$TiO_{2-\delta}N_\delta$(TEA05).

mode of NH_3 [$\delta_s(NH_3)$], respectively}.[91,92] These bands lose their intensities after evacuation at 423 K; in this stage, the difference in the appearance of bands is hardly discernible, compared with that observed in the original stage. This means that nitridation of the sample rarely occurs in this sample, which agrees well with the finding deduced from the data shown above, i.e., low efficiency to nitridation. Heat treatment even at temperatures higher than 473 K results only in small changes in the spectrum.

Quite different patterns of the spectra were observed for the ammonia-treated T-TiO_2(AC) sample. Distinctive bands were observed in the lower-wavenumber region at 1664, 1605, 1435, and 1215 cm^{-1} for the NH_3-adsorbed sample, which was followed by evacuation at 300 K. These bands are associated with the bending vibration modes of coordinated ammonia, molecular water, and ammonium ions that were formed through the adsorption of NH_3. The respective bands are assignable to $\delta_s(NH_4^+)$, $\delta_{as}(NH_3)$, $\delta_{as}(NH_4^+)$, and $\delta_s(NH_3)$, respectively. The band resulting from the bending mode of H_2O [$\delta(H_2O)$] is presumably superimposed upon the band resulting from the asymmetric bending mode of the adsorbed NH_3 because the bending mode of H_2O is observed at around 1620 cm^{-1} in the original sample. The characteristic feature is the appearance of the band at a slightly higher wavenumber at 1215 cm^{-1} for the sample treated at higher temperatures; these spectra exhibited specific new bands at around 1240 cm^{-1}. The curve-fitting procedure for the sample treated at 373 K clearly indicates the existence of two bands, i.e., 1240 and 1215 cm^{-1}, as shown by the result of the curve fitting to the spectrum. The 1240 cm^{-1} band can be explained in terms of the formation of the $-NH_2$ group, $\delta(NH_2)$.[23,91,92] The formation of this band seems to be accompanied by the reduction of the band resulting from the adsorbed NH_3 species (1215 cm^{-1}), which decreases in intensity at a lower temperature compared with the band for the $-NH_2$ species. This behavior seems to be consistent with a decrease in the band intensity at around 1605 cm^{-1}. On the basis of these considerations, the behavior may be related to a change in the coordination structure from $-NH_3$ to $-NH_2$ through heat treatment, although any detailed mechanism for the formation of this band is difficult to formulate at the present stage. The species formed ($-NH_2$) will be followed by incorporation into the T-TiO_2 lattice as nitride or oxynitride, resulting in the formation of T-$TiO_{2-\delta}N_\delta$, the visible-light-based photocatalyst.

4. Photoassisted Reaction by Taking Advantage of Visible Light. Figure 8 shows variation in the absorption spectra of an aqueous solution of MB under irradiation with visible light with $\lambda > 440$ nm for 1 h, when the powders of TiO_2(P-25), nitrided TiO_2(hydrolysis NH_3), and T-$TiO_{2-\delta}N_\delta$ samples were used as photocatalysts. For the TiO_2(P-25) sample, the intensity of the characteristic absorption bands of the MB around 664 nm decreased and finally the solution became colorless when UV light was used as the light source.[93] The powder of the TiO_2 (P-25) sample is known as a catalyst having a relatively high catalytic photoactivity under irradiation with UV light. Once the UV-cutoff filter was inserted in the light path, the photocatalytic activity of the TiO_2(P-25) sample, as well as that of T-TiO_2(AC), was found to be fairly weak; i.e., there was a remarkable decrease in the rate of photodegradation, corresponding well to the fact that the change in the absorption intensity in the visible-light region is almost negligible (spectra given by red and blue lines in Figure 8). When the T-$TiO_{2-\delta}N_\delta(NH_3)$ or $TiO_{2-\delta}N_\delta$(TEA) powder was used as a sample, the photodegradation rate of MB under unfiltered light irradiation was approximately equivalent or lower, compared with that of the TiO_2(P-25) sample alone. A prominent feature was observed for systems in which T-$TiO_{2-\delta}N_\delta(NH_3)$ or $TiO_{2-\delta}N_\delta$(TEA) powder was used as a sample in the experiment when the UV light emitted from a xenon-discharge light was cut by using a filter inserted in the light path; the photobleaching of MB was much faster than that observed for the T-TiO_2(AC), TiO_2(P-25), or nitrided TiO_2 (hydrolysis NH_3) samples (Figure 8). When the light was completely interrupted, the decrease in absorbance became negligible. This process was followed by the restarting of photobleaching through the subsequent irradiation. It is clear from this figure that the degradation reaction proceeded efficiently for the nitride samples depending on the amount of effective nitrogen in the order T-$TiO_{2-\delta}N_\delta$(TEA05) > T-$TiO_{2-\delta}N_\delta$-(TEA01) > T-$TiO_{2-\delta}N_\delta(NH_3)$ > nitrided TiO_2(hydrolysis NH_3) > T-TiO_2(AC) > TiO_2(P-25) under irradiation with visible light ($\lambda >$ 440 nm). Very recently, Ou et al. have reported that the photocatalytic oxidation reaction of phenol over tubular nitrided TiO_2 samples is far superior to that observed on the nitrided TiO_2(P-25) sample, well consistent with our result.[55] On the basis of their result, a similar tendency will also be expected as the results of both the responsiveness to the visible light and the relatively high surface area in our system. In addition, it is noteworthy that the degradation reaction of MB using the present nitride samples shows equal or better performance when compared with the results reported in the experiments carried out under irradiation of the UVA (400−315 nm) or light (346−395 nm) utilizing TiO_2 samples.[94,95] As a result, we can be fairly certain that the nitride T-$TiO_{2-\delta}N_\delta$ samples are working as efficient photocatalysts in the MB decomposition reaction under visible-light-irradiation conditions.

■ CONCLUSIONS

In this experiment, we aimed at preparing the visible-light-derived photocatalyst based on nitridation of a tubular TiO_2 sample having high surface area by utilizing the reaction of the unusual surface acidic sites on the tubular TiO_2 sample with basic molecules having different basicities. In summary, several critical findings in the present experiment are listed as follows:

1 The washing procedure of the prepared tubular TiO_2 sample with an aqueous acidic solution is an indispensable process for the preparation of the nitrided sample with

dx.doi.org/10.1021/ic200424v |Inorg. Chem. 2011, 50, 9948–9957

tubular structure exhibiting an efficient visible-light-derived catalytic property.

2 The acidic nature of the tubular TiO_2 sample washed thoroughly with an aqueous acidic solution was examined by experiments, such as TPD of the adsorbed basic molecules and the catalytic performance utilizing two types of typical reactions including both the ring-opening reaction of an epoxide and a Friedel−Crafts-type reaction. As a result, it is clearly shown that the acid-washed sample exhibits a prominent acidic nature.

3 We succeeded in the preparation of yellow (nitrided) tubular TiO_2 samples with varying amounts of doped nitrogen species through the reaction of the surface sites having an acidic nature, with basic molecules exhibiting different basicities, ammonia and TEA, followed by treatment with dioxygen at 623 K. The tubular structure was retained after such treatment, as shown by experiments such as XRD, TEM, Raman spectroscopy, and collection of the adsorption data.

4 The processes in the nitridation reaction were followed by IR and XPS measurements; first, the acidic OH groups react with NH_3 to form NH_4^+ species, followed by decomposition at higher temperatures, and simultaneous incorporation into the lattice of TiO_2, resulting in the formation of nitrogen-substituted tubular $TiO_{2-\delta}N_\delta$ with high surface area.

5 It is clearly found that the tubular nitrided TiO_2 samples prepared in this experiment function well as efficient photocatalysts for the decomposition of MB in an aqueous solution at 300 K under irradiation with visible light ($\lambda >$ 440 nm), which is different from that observed for the cases using the tubular TiO_2 sample or the P-25 sample, indicating the efficient attainment of visible-light responsiveness on the tubular TiO_2 sample through treatment with ammonia or TEA.

■ ASSOCIATED CONTENT

Supporting Information. Experimental procedures related to catalytic performances of the samples are given in SI: surface acidic nature examined by the TPD method utilizing TCD as a detector given as spectra (Figure S1), IR spectra of adsorbed CO species on tubular TiO_2 samples (Figure S2), both adsorption isotherms of N_2 on various samples and the resulting pore-size distribution data (Figure S3), and Raman spectra of various samples (Figure S4). This material is available free of charge via the Internet at http://pubs.acs.org.

■ AUTHOR INFORMATION

Corresponding Author

*E-mail: kuroda@cc.okayama-u.ac.jp. Phone and fax: +81-86-251-7844.

■ ACKNOWLEDGMENT

This project was partially supported by a Grant-in-Aid from the Ministry of Education, Culture, Sports, Science, and Technology of Japan (Grant 17GS0206). We also thank both Iketani Science and Technology and Hosokawa Powder Technology Foundations for their generous financial assistance. The authors wish to express their appreciation to Dr. T. Funamoto (Research Institute Center, Okayama University of Science) for his valuable comments and for his cooperation in the XPS measurements. Thanks are also due to BEL Inc. (Japan) for supporting us in the experiment of the TPD-MS measurements. Y.H. acknowledges financial support for his research in a doctoral course from Okayama University.

■ REFERENCES

(1) Fujishima, A.; Honda, K. *Bull. Chem. Soc. Jpn.* **1971**, *44*, 1148–1150.
(2) Fujishima, A.; Honda, K. *Nature* **1972**, *238*, 37–38.
(3) Fujishima, A.; Zhang, X.; Tryk, D. A. *Surf. Sci. Rep.* **2008**, *63*, 515–582.
(4) Linsebigler, A.; Lu, G.; Yates, J. T., Jr. *Chem. Rev.* **1995**, *95*, 735–758.
(5) Diebold, U. *Surf. Sci. Rep.* **2003**, *48*, 53–229.
(6) Ghosh, A. K.; Maruska, H. P. *J. Electrochem. Soc.* **1977**, *124*, 1516–1522.
(7) Borgarello, E.; Kiwi, J.; Graetzel, M.; Pelizzetti, E.; Visca, M. V. *J. Am. Chem. Soc.* **1982**, *104*, 2996–3002.
(8) Hermann, J.-M.; Disdier, J.; Pichat, P. *Chem. Phys. Lett.* **1984**, *108*, 618–622.
(9) Serpone, N.; Lawless, D.; Disdier, J.; Herrmann, J.-M. *Langmuir* **1994**, *10*, 643–652.
(10) Ikeda, S.; Sugiyama, N.; Pal, B.; Marci, G.; Palmisano, L.; Noguchi, H.; Uosaki, K.; Ohtani, B. *Phys. Chem. Chem. Phys.* **2001**, *3*, 267–273.
(11) Irie, H.; Miura, S.; Kamiya, K.; Hashimoto, K. *Chem. Phys. Lett.* **2008**, *457*, 202–205.
(12) Nakamura, I.; Negishi, N.; Kutsuna, S.; Ihara, T.; Sugihara, S.; Takeuchi, K. *J. Mol. Catal. A: Chem.* **2000**, *161*, 205–212.
(13) Hossain, F. M.; Murch, G. E.; Sheppard, L.; Nowotny, J. *Solid State Ionics* **2007**, *178*, 319–325.
(14) Khan, S. U. M.; Al-Shahry, M. W.; Ingler, W. B., Jr. *Science* **2002**, *297*, 2243–2245.
(15) Irie, H.; Watanabe, Y.; Hashimoto, K. *Chem. Lett.* **2003**, *32*, 772–773.
(16) Sakthivel, S.; Kisch, H. *Angew. Chem., Int. Ed.* **2003**, *42*, 4908–4911.
(17) Tachikawa, T.; Tojo, S.; Kawai, K.; Endo, M.; Fujitsuka, M.; Ohno, T.; Nishijima, K.; Miyamoto, Z.; Majima, T. *J. Phys. Chem. B* **2004**, *108*, 19299–19306.
(18) Sato, S. *Chem. Phys. Lett.* **1986**, *123*, 126–128.
(19) Asahi, R.; Morikawa, T.; Ohwaki, T.; Aoki, K.; Taga, Y. *Science* **2001**, *293*, 269–271.
(20) Burda, C.; Lou, Y.; Chen, X.; Samia, A. C. S.; Stout, J.; Gole, J. L. *Nano Lett.* **2003**, *3*, 1049–1051.
(21) Zhao, Y.; Qiu, X.; Burda, C. *Chem. Mater.* **2008**, *20*, 2629–2636.
(22) Irie, H.; Watanabe, Y.; Hashimoto, K. *J. Phys. Chem. B* **2003**, *107*, 5483–5486.
(23) Kuroda, Y.; Mori, T.; Yagi, K.; Makihata, N.; Kawahara, Y.; Nagao, M.; Kittaka, S. *Langmuir* **2005**, *21*, 8026–8034.
(24) Di Valentin, C.; Pacchioni, G.; Selloni, A.; Livraghi, S.; Giamello, E. *J. Phys. Chem. B* **2005**, *109*, 11414–11419.
(25) Livraghi, S.; Paganini, M. C.; Giamello, E.; Selloni, A.; Valentin, C. D.; Pacchioni, G. *J. Am. Chem. Soc.* **2006**, *128*, 15666–15671.
(26) Chen, H.; Nambu, A.; Wen, W.; Graciani, J.; Zhong, Z.; Hanson, J. C.; Fujita, E.; Rodriguez, J. A. *J. Phys. Chem. C* **2007**, *111*, 1366–1372.
(27) Yang, X.; Cao, C.; Erickson, L.; Hohn, K.; Maghirang, R.; Klabunde, K. *J. Catal.* **2008**, *260*, 128–133.
(28) Subbarao, S. N.; Yun, Y. H.; Kershaw, R.; Dwinght, K.; Wold, A. *Inorg. Chem.* **1979**, *18*, 488–492.
(29) Yamaki, T.; Sumita, T.; Yamamoto, S. *J. Mater. Sci. Lett.* **2002**, *21*, 33–35.
(30) Nukumizu, K.; Nunoshige, J.; Takata, T.; Kondo, J. N.; Hara, M.; Kobayashi, H.; Domen, K. *Chem. Lett.* **2003**, *32*, 196–197.
(31) Li, D.; Haneda, H.; Labhsetwar, N. K.; Hishita, S.; Ohashi, N. *Chem. Phys. Lett.* **2005**, *401*, 579–584.

(32) Umebayashi, T.; Yamaki, T.; Itoh, H.; Asai, K. *Appl. Phys. Lett.* **2002**, *81*, 454–456.
(33) Tada, H.; Mitsui, T.; Kiyonaga, T.; Akita, T.; Tanaka, K. *Nat. Mater.* **2006**, *5*, 782–786.
(34) Miyauchi, M.; Nakajima, A.; Hashimoto, K.; Watanabe, T. A. *Adv. Mater.* **2000**, *12*, 1923–1927.
(35) Simon, P.; Pignon, B.; Miao, B.; Coste-Leconte, S.; Leconte, Y.; Marguet, S.; Jegou, P.; Bouchet-Fabre, B.; Reynaud, C.; Herlin-Boime, N. *Chem. Mater.* **2010**, *22*, 3704–3711.
(36) György, E.; Pérez del Pino, A.; Serra, P.; Morenza, J. L. *Appl. Surf. Sci.* **2002**, *186*, 130–134.
(37) Guillot, J.; Chappé, J.-M.; Heintz, O.; Martin, N.; Imhoff, L.; Takadoum, J. *Acta Mater.* **2006**, *54*, 3067–3074.
(38) Ghicov, A.; Macak, J. M.; Tsuchiya, H.; Kunze, J.; Haeublein, V.; Kleber, S.; Schmuki, P. *Chem. Phys. Lett.* **2006**, *419*, 426–429.
(39) Diwald, O.; Thompson, T. L.; Goralski, E. G.; Walck, S. D.; Yates, J. T., Jr. *J. Phys. Chem. B* **2004**, *108*, 52–57.
(40) Sakthivel, S.; Kisch, H. *ChemPhysChem.* **2003**, *4*, 487–490.
(41) Diwald, O.; Thompson, T. L.; Zubkov, T.; Goralski, E. G.; Walck, S. D.; Yates, J. T., Jr. *J. Phys. Chem. B* **2004**, *108*, 6004–6008.
(42) Torres, G. R.; Lindgren, T.; Lu, J.; Granqvist, C.-G.; Lindquist, S.-E. *J. Phys. Chem. B* **2004**, *108*, 5995–6003.
(43) Mrowetz, M.; Balcerski, W.; Colussi, A. J.; Hoffmann, M. R. *J. Phys. Chem. B* **2004**, *108*, 17269–17273.
(44) Nakamura, R.; Tanaka, T.; Nakato, Y. *J. Phys. Chem. B* **2004**, *108*, 10617–10620.
(45) Joung, S.-K.; Amemiya, T.; Murabayashi, M.; Itoh, K. *Chem.—Eur. J.* **2006**, *12*, 5526–5534.
(46) Yang, S.; Gao, L. *J. Am. Ceram. Soc.* **2004**, *87*, 1803–1805.
(47) Miyauchi, M.; Ikezawa, A.; Tobimatsu, H.; Irie, H.; Hashimoto, K. *Phys. Chem. Chem. Phys.* **2004**, *6*, 865–870.
(48) Randeniya, L. K.; Bendavid, A.; Martin, P. J.; Preston, E. W. *J. Phys. Chem. C* **2007**, *111*, 18334–18340.
(49) Tokudome, H.; Miyauchi, M. *Chem. Lett.* **2004**, *33*, 1108–1109.
(50) Rhee, C. H.; Lee, J. S.; Chung, S. H. *J. Mater. Res.* **2005**, *20*, 3011–3020.
(51) Feng, C.; Wang, Y.; Jin, Z.; Zhang, J.; Zhang, S.; Wu, Z.; Zhang, Z. *New J. Chem.* **2008**, *32*, 1038–1047.
(52) Jiang, Z.; Yang, F.; Luo, N.; Chu, B. T. T.; Sun, D.; Shi, H.; Xiao, T.; Edwards, P. P. *Chem. Commun.* **2008**, 6372–6374.
(53) Geng, J.; Yang, D.; Zhu, J.; Chen, D.; Jiang, Z. *Mater. Res. Bull.* **2009**, *44*, 146–150.
(54) Kitano, M.; Nakajima, K.; Kondo, J. N.; Hayashi, S.; Hara, M. *J. Am. Chem. Soc.* **2010**, *132*, 6622–6623.
(55) Ou, H.-H.; Lo, S.-L.; Liao, C.-H. *J. Phys. Chem. C* **2011**, *115*, 4000–4007.
(56) Kasuga, T.; Hiramatsu, M.; Hoson, A.; Sekino, T.; Niihara, K. *Adv. Mater.* **1999**, *11*, 1307–1311.
(57) Kasuga, T.; Hiramatsu, M.; Hoson, A.; Sekino, T.; Niihara, K. *Langmuir* **1998**, *14*, 3160–3163.
(58) Menzel, R.; Peiró, A. M.; Durrant, J. R.; Shaffer, M. S. P. *Chem. Mater.* **2006**, *18*, 6059–6068.
(59) Morgado, E., Jr.; Abreu, M. A. S.; Moure, T. G.; Marinkovic, B. A.; Jardim, P. M.; Araujo, A. S. *Chem. Mater.* **2007**, *19*, 665–676.
(60) Bavykin, D. V.; Friedrich, J. M.; Walsh, F. C. *Adv. Mater.* **2006**, *18*, 2807–2824.
(61) Morgan, D. L.; Liu, H.-W.; Frost, R. L.; Waclawik, E. R. *J. Phys. Chem. C* **2010**, *114*, 101–110.
(62) Cesano, F.; Bertarione, S.; Uddin, M. S.; Agostini, G.; Scarano, D.; Zecchina, A. *J. Phys. Chem. C* **2010**, *114*, 169–178.
(63) Bavykin, D. V.; Gordeev, S. N.; Moskalenko, A. V.; Lapkin, A. A.; Walsh, F. C. *J. Phys. Chem. B* **2005**, *109*, 8565–8569.
(64) Eder, D.; Kinloch, I. A.; Windle, A. H. *Chem. Commun.* **2006**, 1448–1450.
(65) Tsai, C.-C.; Teng, H. *Chem. Mater.* **2004**, *16*, 4352–4358.
(66) Richter, C.; Wu, Z.; Panaitescu, E.; Willey, R. J.; Menon, L. *Adv. Mater.* **2007**, *19*, 946–948.
(67) Kim, S.-J.; Yun, Y.-U.; Oh, H.-J.; Hong, S. H.; Roberts, C. A.; Routray, K.; Wachs, I. E. *J. Phys. Chem. Lett.* **2010**, *1*, 130–135.
(68) Wagner, C. D.; Riggs, W. M.; Davis, L. E.; Moulder, J. F.; Mullenberg, G. E. In *Handbook of X-ray Photoelectron Spectroscopy*; Prairie, E., Ed.; Perkin-Elmer: Minneapolis, MN, 1979.
(69) Katada, N.; Suzuki, K.; Noda, T.; Park, M. B.; Min, H.-K.; Hong, S. B.; Niwa, M. *Top. Catal.* **2010**, *53*, 664–671.
(70) Farneth, W. E.; Gorte, R. J. *Chem. Rev.* **1995**, *95*, 615–635.
(71) Mori, T.; Kuroda, Y.; Yoshikawa, Y.; Nagao, M.; Kittaka, S. *Langmuir* **2002**, *18*, 1595–1603.
(72) Raj, K. J. A.; Viswanathan, B. *Indian J. Chem.* **2009**, *48A*, 1378–1382.
(73) Gao, T.; Fjellvåg, H.; Norby, P. *Inorg. Chem.* **2009**, *48*, 1423–1432.
(74) Kolen'ko, Y. V.; Kovnir, K. A.; Gavrilov, A. I.; Garshev, A. V.; Frantti, J.; Lebedev, O. I.; Churagulov, B. R.; Tendeloo, G. V.; Yoshimura, M. *J. Phys. Chem. B* **2006**, *110*, 4030–4038.
(75) Gajović, A.; Friščić, I.; Plodinec, M.; Iveković, D. *J. Mol. Struct.* **2009**, *924−926*, 183–191.
(76) Hendrickson, D. N.; Hollander, J. M.; Jolly, W. L. *Inorg. Chem.* **1969**, *8*, 2642–2647.
(77) Chen, C.; Bai, H.; Chang, C. *J. Phys. Chem. C* **2007**, *111*, 15228–15235.
(78) Chen, X.; Wang, X.; Hou, Y.; Huang, J.; Wu, L.; Fu, X. *J. Catal.* **2008**, *255*, 59–67.
(79) Shi, Z. M.; Ye, X. Y.; Liang, K. M.; Gu, S. R.; Pan, F. *J. Mater. Sci. Lett.* **2003**, *22*, 1255–1258.
(80) Saha, N. C.; Tompkins, H. G. *J. Appl. Phys.* **1992**, *72*, 3072–3079.
(81) Gole, J. L.; Stout, J. D.; Burda, C.; Lou, Y.; Chen, X. *J. Phys. Chem. B* **2004**, *108*, 1230–1240.
(82) Chen, X.; Burda, C. *J. Phys. Chem. B* **2004**, *108*, 15446–15449.
(83) Chen, X.; Lou, Y.; Samia, A. C. S.; Burda, C.; Gole, J. L. *Adv. Funct. Mater.* **2005**, *15*, 41–49.
(84) Prokes, S. M.; Gole, J. L.; Chen, X.; Burda, C.; Carlos, W. E. *Adv. Funct. Mater.* **2005**, *15*, 161–167.
(85) Ghicov, A.; Macak, J. M.; Tsuchiya, H.; Kunze, J.; Haeublein, V.; Frey, L.; Schmuki, P. *Nano Lett.* **2006**, *6*, 1080–1082.
(86) Sathish, M.; Viswanathan, B.; Viswanath, R. P.; Gopinath, C. S. *Chem. Mater.* **2005**, *17*, 6349–6353.
(87) Di Valentin, C.; Finazzi, E.; Pacchioni, G.; Selloni, A.; Livraghi, S.; Paganini, M. C.; Giamello, E. *Chem. Phys.* **2007**, *339*, 44–56.
(88) Baltrusaitis, J.; Jayaweera, P. M.; Grassian, V. H. *Phys. Chem. Chem. Phys.* **2009**, *11*, 8295–8305.
(89) Nosaka, Y.; Matsushita, M.; Nishino, J.; Nosaka, A. Y. *Sci. Technol. Adv. Mater.* **2005**, *6*, 143–148.
(90) Wang, J.; Tafen, D. N.; Lewis, J. P.; Hong, Z.; Manivannan, A.; Zhi, M.; Li, M.; Wu, N. *J. Am. Chem. Soc.* **2009**, *131*, 12290–12297.
(91) Hadjiivanov, K.; Sauer, O.; Lamotte, J.; Lavalley, J.-C. *Z. Phys. Chem.* **1994**, *187*, 281–300.
(92) Ramis, G.; Yi, L.; Busca, G. *Catal. Today* **1996**, *28*, 373–380.
(93) De Tacconi, N. R.; Carmona, J.; Rajeshwar, K. *J. Electrochem. Soc.* **1997**, *144*, 2486–2490.
(94) Zita, J.; Krýsa, J.; Mills, A. *J. Photochem. Photobiol., A* **2009**, *203*, 119–124.
(95) Random, C.; Wongnawa, S.; Boonsin, P. *ScienceAsia* **2004**, *30*, 149–156.